THE ASTROPHYSICAL JOURNAL, 218: 736–748, 1977 December 15

MOLECULAR CLOUDS AND STAR FORMATION. I. OBSERVATIONS OF THE CEPHEUS OB3 MOLECULAR CLOUD

ANNEILA I. SARGENT
Hale Observatories, California Institute of Technology, Carnegie Institution of Washington
Received 1977 April 18; accepted 1977 June 10

ABSTRACT

To determine the connection between newly formed stars and molecular clouds, observations were made in and around the young OB association Cepheus OB3 in the $J = 1 \rightarrow 0$ transition of ^{12}CO. An extended (20 pc × 60 pc) molecular cloud was detected and mapped, and additional observations of ^{13}CO and H_2CO were made at selected positions. Moderately enhanced temperatures and densities were noted in several portions of the cloud. It appears that star formation is still continuing in the Cepheus OB3 complex.

Subject headings: interstellar: molecules — nebulae: individual — stars: formation

I. INTRODUCTION

It is well established that newly formed stars are frequently found in association with dense molecular clouds. Among the better-known examples are the infrared cluster in Orion (Becklin, Neugebauer, and Wynn-Williams 1973; Liszt *et al.* 1974); the infrared sources and water maser found at the edge of the M17 cloud (Lada 1976; Elmegreen and Lada 1977); the compact H II regions, H_2O masers, OH masers, and infrared sources located along the boundary of the molecular cloud connected with W3 (Mezger and Wink 1975; Harris and Wynn-Williams 1976), and the infrared objects, compact H II regions, H_2O masers, and OH masers found in the region of the Mon R2 cloud (Downes *et al.* 1975; Kutner and Tucker 1975; Beckwith *et al.* 1976).

However, the way in which stars form within these clouds and the subsequent behavior of the clouds themselves are not well understood. In particular, if it is assumed that all molecular clouds collapse gravitationally to form stars, the resulting star-formation rate is much greater than that observed (cf. Zuckerman and Palmer 1974). For the predicted and observed rates to agree, it is necessary either that contraction take place on a time scale longer than that for free-fall collapse or that only a fraction of the cloud material form stars.

To elucidate the relationship between star formation and molecular clouds, a detailed analysis of some group of newly formed stars and a related molecular cloud is required. To this end, two such groups, Cepheus OB3 and Perseus OB2, were selected, and associated molecular clouds were searched for, detected, and mapped in the 115 GHz line of carbon monoxide. Sizes and masses of the clouds were determined from measurements of both the ^{12}CO and ^{13}CO lines, while their structure was investigated through the variation with position of line widths, temperatures, and velocities.

In view of the abundance of available data and the extensive molecular observations involved in the current study, this paper will confine itself to a presentation of the observations of Cepheus OB3 only. Observations of Perseus OB2 will be described in Paper II (Sargent 1978*a*), and detailed interpretation of these data will be made in Paper III (Sargent 1978*b*).

II. OBSERVATIONAL SELECTION

The young OB association Cepheus OB3 was selected primarily because it is young enough to be a site of recent star formation (its youngest stars are of age $\sim 4 \times 10^6$ years, comparable to the youngest optically visible stars in Orion OB1), but is also sufficiently old that its primeval cloud must have evolved to some extent. Its basic properties are described in Blaauw's (1964) list of O associations in the solar neighborhood.

Cepheus OB3 is composed of two subgroups (see Fig. 1) of stars; the older is of age 8×10^6 years and the younger, 4×10^6 years. This typical age difference between individual subgroups of an OB association suggests that there will be indications within any adjacent clouds of the beginnings of yet another epoch of stellar birth. At 730 pc the association is sufficiently close that the detection and measurement of infrared sources, molecular peaks, and other signposts of protostars are facilitated.

The difference between the masses of OB associations ($\sim$few $\times 10^3 M_\odot$) and typical molecular clouds ($\sim 10^4$–$10^5 M_\odot$) can be explained if only a fraction of the cloud material forms stars. Thus analysis of the structure of a molecular cloud after some star formation has taken place may indicate the subsequent behavior of the cloud material and in particular whether it eventually disperses. Blaauw noted, and it is clear from inspection of the Palomar Sky Atlas, that the degree to which interstellar matter permeates OB associations decreases with association age. As might be expected, a considerable amount of interstellar material is still present in the vicinity of Cepheus OB3, so that the region is particularly suitable for studying this question of cloud evolution.

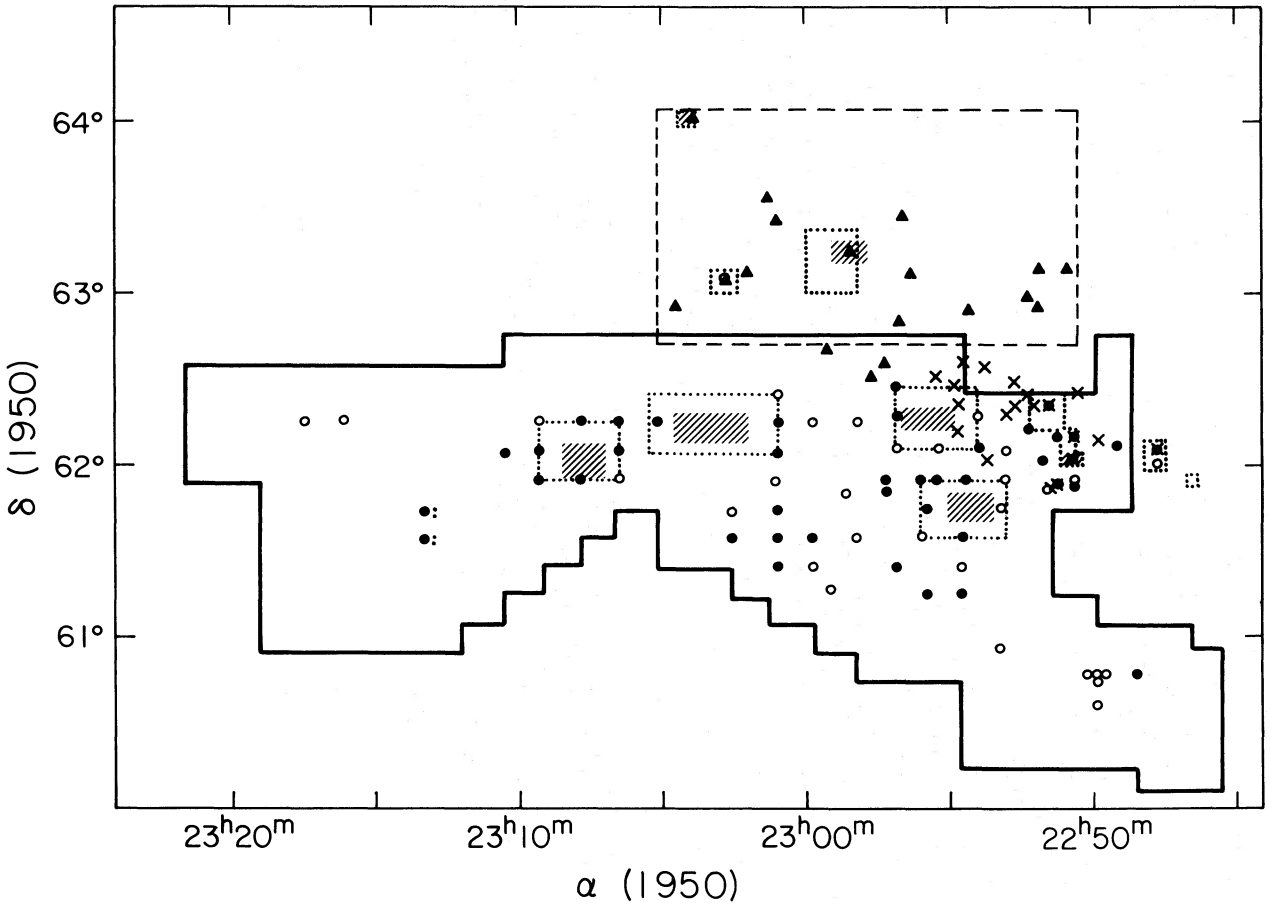

FIG. 1.—Areas of the sky covered by observations at various separations. A heavy solid line outlines the region where ^{12}CO measurements at 10′ spacings were made; 2′ and 20′ sampled areas are bounded by dotted and dashed lines, respectively. Measurements of ^{13}CO at 2′ spacings were made over the hatched zones. Other ^{13}CO observations are indicated by filled circles where the isotope was detected and by open circles where it was absent. The stars of the association are represented by crosses and filled triangles; crosses denote members of the younger subgroup, and filled triangles, members of the older subgroup of Cepheus OB3.

This association has the further advantage that the properties of its stars have already been investigated in some detail. Proper motions, association membership, and radial velocities of the stars, as well as expansion velocities of the two subgroups in Cepheus OB3, have been determined by Garmany (1973). Spectral classes on the MK system were assigned by Garrison (1970) in the course of an investigation of total to selective absorption across the association. The stars have been well studied photometrically, from the original *UBV* measurements of Blaauw, Hiltner, and Johnson (1959), through the *ubvy* and Hβ photometry of Crawford and Barnes (1970), to the ultraviolet observations of the ANS instrument (Kester 1977). In addition, an area of considerable extent ($l = 90°$ to 115°, $b = -1°$ to $+15°$) around and including Cepheus OB3 was surveyed in the 21 cm line of neutral hydrogen by Simonson and van Someren Greve (1976). They derived a possible model of the OB association with respect to the surrounding neutral hydrogen. Finally, to augment this already large pool of data, a search has been made by Harris (1976), in conjunction with the observations described here, for compact H II regions in the neighborhood of S155, the H II region located in the southwest of Cepheus OB3.

III. CO OBSERVATIONS

The 4.6 m telescope of the Aerospace Corporation in El Segundo, California, was used to map a 1°.5 × 4°.5 area of Cepheus in the $J = 1 \rightarrow 0$ transitions of ^{12}CO(115 GHz) and ^{13}CO(110 GHz). The telescope has a main beam efficiency of 70% and a half-power beamwidth of 2′.5. Most observations were obtained between 1975 December and 1976 March when weather conditions were excellent, with zenith optical depths of ~0.3 at 115 GHz and ~0.2 at 110 GHz. Typical integration times of 10 minutes for ^{12}CO and 15 minutes for ^{13}CO were used. The single sideband system temperature at CO frequencies using an uncooled mixer receiver was ~1200 K. Spectral lines

were detected with a 64 channel filter bank giving a resolution of 250 kHz (0.65 km s^{-1} at 115 GHz) per channel. Baseline stability was achieved by frequency switching with 8 MHz separation between signal and reference bands. The reference line was inverted with respect to the signal and later folded with it, thereby effectively increasing the integration time. The corrected antenna temperature, T_A^*, is the temperature measured by a lossless antenna above the Earth's atmosphere, where

$$T_A^* = \frac{h\nu}{k}\left[F(T_B) - F(T_{bb})\right],$$

and

$$F(T) = \left[\exp\frac{h\nu}{kT} - 1\right]^{-1}.$$

T_B is the source brightness temperature and T_{bb} is the temperature of the microwave background. To determine T_A^*, the signal observed on-source is corrected for atmospheric attenuation by multiplying by a factor of exp (τ_0 sec z), where z is the zenith distance of the source observed and τ_0 is the zenith optical depth. Measurements of τ_0 by tipping were made every 3 or 4 hours during each observing session. This corrected signal is scaled to the system temperature by using an observing chopper at 300 K which rotated in the field of view of the feed horn. As a further check on the stability of the system, Orion A was observed each day and one point of relatively strong CO emission within the cloud was monitored each hour throughout all observing runs. The final values of T_A^* are on a scale such that for Orion A $T_A^*(^{12}CO) = 70$ K and $T_A^*(^{13}CO) = 10.9$ K.

a) ^{12}CO

Observations of ^{12}CO were first made at spacings of 10′ (i.e., four beamwidths) in right ascension and declination. Mapping was continued until the boundaries of the cloud (defined as $T_A^* \leq 2.5$ K) could be specified.

A primary concern of the survey was to detect small-scale structure in the clouds and, in particular, to determine the location of possible sites of star formation. Since lines exhibiting enhanced temperatures, wide wings, or a considerable degree of broadening are indicators of such sites, more detailed measurements at spacings of 2′ in right ascension and declination were made about any profile which displayed these properties. The usual criterion for use of this finer grid was that $T_A^* \geq 10$ K. This criterion incidentally selected regions displaying broadened or wide-winged lines for finer grid measures.

Observations were also made in the directions of the OB association members. Mapping was carried out around a few of the younger subgroup stars, several of which lie within the cloud boundaries. Gas was unambiguously detected in the direction of only one older subgroup member. In a few doubtful cases, measurements were made as indicated in Figure 1. As a further check for the presence of CO outside the primary cloud boundaries, but in the general vicinity of the association stars, observations at 20′ spacings were made along the length of the cloud and perpendicular to it beyond the declination of the most northerly association member. The area encompassed by these observations is shown in Figure 1.

b) ^{13}CO

Observations of the rarer isotope were for the most part confined to the vicinity of the "hot spots" as determined by the ^{12}CO survey. Other detailed measurements were made (see Fig. 1) in the neighborhood of the association stars 11, 56, and 75. The numbering system adopted is that of Blaauw, Hiltner, and Johnson (1959). An effort was made to continue observations of the hot spots outward from a central position until $T_A^*(^{13}CO) \leq 1$ K. In some directions further observations were made at distances of 10′ from the central position in the hope of estimating the extent of the presence of ^{13}CO. The results will be discussed in § V*b*. Figure 1 illustrates how far this procedure was employed. Further ^{13}CO observations were made where broadened or multiple lines were seen in ^{12}CO. In cases where the ^{13}CO line was detected to be at least 3 K, some large-scale mapping was carried out.

c) *High-Resolution Measurements*

Observations at higher spatial resolution are needed to clarify the nature of hot spots found in the initial Aerospace survey. These hot spots were therefore studied at ^{12}CO and ^{13}CO frequencies, using the 11 m telescope of the National Radio Astronomy Observatory at Kitt Peak, Arizona,[1] in conjunction with the 256 × 100 kHz and 256 × 250 kHz filter banks. The single sideband system temperature was ~1000 K, while the half-power beamwidth is ~65″ at 115 GHz. Similar calibration procedures to those at Aerospace were employed. Values of T_A^* are on a scale such that for Orion A $T_A^*(^{12}CO) = 60$ K (Ulich and Haas 1976). The telescope was operated in the position-switching mode. Off-source positions were typically 30′ away from the source, at locations previously determined to be free of CO emission. Useful, high-resolution profiles were obtained, but detailed measurements about the positions of peak T_A^* are very limited. Both with respect to line shape and to peak T_A^* observed, these profiles are in excellent agreement with those obtained in the same directions but at lower resolution at Aerospace.

IV. FORMALDEHYDE OBSERVATIONS

Since the presence of the $J_{K-K+} = 2_{12} \rightarrow 1_{11}$ transition of formaldehyde is often associated with relatively high molecular hydrogen densities (n_{H_2} = 10^4–10^5 cm^{-3}) (Lucas, Encrenaz, and Falgarone 1976, and references therein), a search was made at and

[1] The National Radio Astronomy Observatory is operated by Associated Universities for Research in Astronomy, Inc., under contract with the National Science Foundation.

around the positions of the hot spots for this 140 GHz line. The observations were made in 1976 March and 1976 May with the 5 m telescope of the Millimeter Wave Observatory, Fort Davis, Texas,[2] operated in a frequency-switching mode. The single sideband system temperature for H_2CO was 2400 K, and the half-power beamwidth 2′. The spectral resolution was 0.53 km s^{-1}. Calibration was carried out by the usual chopper wheel technique. Orion A, with $T_A^*(H_2CO) = 4.8$ K, was observed daily to establish a standard comparison. Measurements were made at spacings of 2′ around the positions of peak intensity to determine the sizes of the H_2CO emission regions.

V. RESULTS

a) ^{12}CO

The velocity at which peak antenna temperature, $T_A^*(^{12}CO)$, occurs is not the same throughout the cloud, but ranges from -5 km s^{-1} to -15 km s^{-1}; the peak emission appears most frequently at velocities around -10 km s^{-1}. In Figure 2 are shown contours of peak $T_A^*(^{12}CO)$ within this velocity range. The elongation of the molecular cloud parallel to the galactic plane is particularly marked. Positions of the association stars with respect to the cloud are also displayed in this figure; the older subgroup is represented by filled triangles and the younger by crosses. To facilitate later discussion, regions of the cloud which will be referred to individually have been designated A, B, C, etc., in the figure. In Figure 3 (Plate 22), the contours of $T_A^*(^{12}CO)$ as shown in Figure 2 are superposed on the Palomar Sky Survey (PSS) print of the Cepheus region. The contours of Cep B partially obscure the H II region S155.

The maps of Cep A, B, C, D, and E derived from higher positional sampling were found to be in good agreement with those determined from mapping at 10′ × 10′ spacings. Limited 2′ × 2′ mapping of Cep F, however, indicates the presence of small-scale structure not shown in Figure 2. Several of the younger association members lie within the boundaries of Cep F, and it is possible that the differences between the results of the 10′ × 10′ survey and the 2′ × 2′ measures are attributable to the presence of these stars.

A few isolated observations around $\alpha = 22^h47^m$, $\delta = 62°00'$ (cf. Fig. 1) near an association star reveal the presence of CO at a velocity appropriate to the primary cloud. From examination of the PSS print and the available measurements, it seems likely that this secondary component is fairly small, perhaps comparable with Cep B in size. The highest values of $T_A^*(^{12}CO)$ noted are of the order of 10 K. Further

[2] The Millimeter Wave Observatory is operated by the Electrical Engineering Research Laboratory of the University of Texas at Austin.

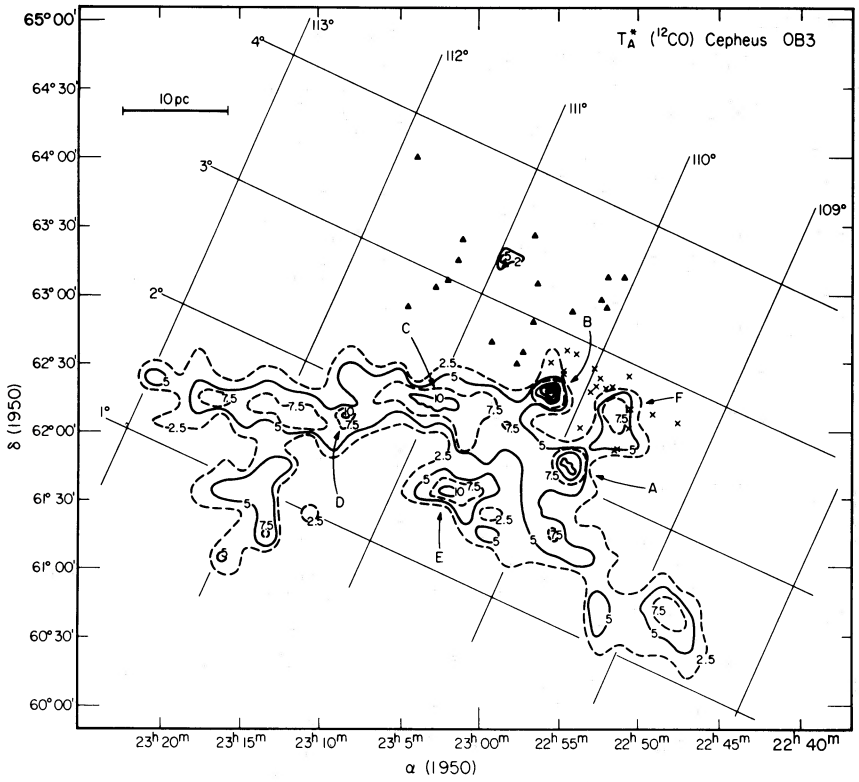

FIG. 2.—Contours of peak antenna temperature, $T_A^*(^{12}CO)$. As in Fig. 1, the crosses and triangles symbolize the association stars. Areas Cep A, B, C, D, E, and F, discussed in the text, are indicated. At Cep A and B the undesignated contours represent values of T_A^* increasing from 10 K to 25 K by increments of 5 K.

mapping of this zone and of Cep F is clearly important.

Across large areas of the Cepheus cloud, double, and frequently triple, features are visible in the ^{12}CO profiles. Maps of T_A^* at a number of velocities between -5 km s^{-1} and -12 km s^{-1} were therefore constructed and are displayed in Figures 4*a* through 4*e*. The T_A^* plotted is the highest value of that quantity noted within ± 0.65 km s^{-1} of the velocity quoted for each map. For comparison, Figure 2 is redrawn to the same scale alongside these figures. Maps were not produced at $V_{LSR} \approx -7$ km s^{-1} or $V_{LSR} < -12$ km s^{-1} where peaks in T_A^* occur only rarely. Evidently the cloud comprises a number of components at different velocities, each of which follows to some degree the overall elongated pattern noted above.

It is evident from a comparison of Figures 4*a* through 4*e* and Figure 2 that the strongest emission from the region of the cloud closest to the association stars occurs at velocities near -12 km s^{-1}. The feature observed at this velocity falls off in intensity quite rapidly, to be replaced by emission closer to -10.7 km s^{-1}, particularly in the vicinity of Cep A, Cep C, and Cep E. Emission at more positive velocities tends on the whole to be patchily distributed, or at least seems uncorrelated with the positions of either the hot spots or the stars.

The range of cloud velocities observed here is well within the range of the association stellar velocities. The stars have values of V_{LSR}, measured with typical errors of ± 5 km s^{-1}, extending in value from 0 km s^{-1} to -30 km s^{-1}, with a mean of -11 km s^{-1} (Garmany 1973; see also Simonson and van Someren Greve 1976). For the 11 younger association members for which radial velocities are available, the mean is ~ -15 km s^{-1}. The V_{LSR} of the H II region S155, determined by Miller (1968) from the Hα line on standard slit spectrograms, and by Georgelin (1975) from photographic Fabry-Perot interferometry, is also -15 km s^{-1}. Errors quoted are typically 4–8 km s^{-1}. In view of the excellent agreement between results acquired by such widely differing techniques, it is presumed that some confidence may be placed in the value -15 km s^{-1}. It is notable that in Cep B, the region of the molecular cloud closest to S155, strong ^{12}CO emission occurs at a very similar velocity, -12 km s^{-1}.

Several of the younger association members lie in the direction of or close to Cep F. As may be seen from Table 1, only stars 11 and 24 have radial velocities close to those at which emission is detected from the cloud. In the direction and at the velocity of both these stars, the CO emission is decidedly weak (almost at the limit of detectability for 24) and quite localized. In general, emission from Cep F occurs between -8 km s^{-1} and -9 km s^{-1} (see Figs. 4*c*, 4*d*), but close to stars 11 and 24 the line profiles are distorted toward more negative velocities, presumably as a result of contamination by gas associated with the stars. Occasionally CO was seen near, but not precisely in the direction of, a stellar position. In these cases a designation in Table 1 such as 17–8S 4E indicates a position 8′ south and 4′ east of star 17.

With the exception of star 56 and possibly star 75, there is no evidence for the existence of CO in the direction of older subgroup members of Cepheus OB3. Within the primary cloud emission at such negative velocities (see Table 1) is only observed close to the northwestern boundary.

To summarize, ^{12}CO emission at more negative velocities (i.e., ≤ -12 km s^{-1}) tends to be confined to the northern edges of the cloud around Cep B, S155, and close to the association stars; in the regions of broadened lines (e.g., Cep A, Cep C) where future star formation may be expected to take place (see §§ VI, VII), peak T_A^* occurs at less negative velocities, between -10 km s^{-1} and -11 km s^{-1}; emission at more positive velocities arises from what seem to be fairly tenuous extended regions in which there are as yet no indications of star formation.

b) ^{13}CO

In the Cepheus molecular cloud ^{13}CO was detected in Cep A, B, C, and D and at the positions indicated by filled circles in Figure 1. Detailed contour maps of $T_A^*(^{13}CO)$ for Cep A, B, and C are presented in the sections dealing specifically with these regions (see § IV). Observations at the locations of Cep E and

TABLE 1

VELOCITIES OF CO EMISSION AT AND NEAR ASSOCIATION STARS

Position*	α(1950)	δ(1950)	V_{LSR} (star)† (km s^{-1})	V_{LSR} (CO) (km s^{-1})
2—4S	22^{h}47^{m}42^s	+62°00′04″	+1	−12
10—4E	22 51 08	+62 10 29	−23	−10
11	22 50 37	+62 02 50	−13	−11
15	22 51 18	+61 52 46	−29	−9
16	22 51 33	+61 52 07	−22	−10
17—8S 4E	22 52 11	+62 12 48	...	−9
24	22 52 39	+62 20 44	−12	−12:
56	22 58 33	+63 14 52	−14	−14
75	23 03 56	+64 01 30	−13	−15:

* Star numbers from Blaauw, Hiltner, and Johnson 1959.

† Garmany 1973.

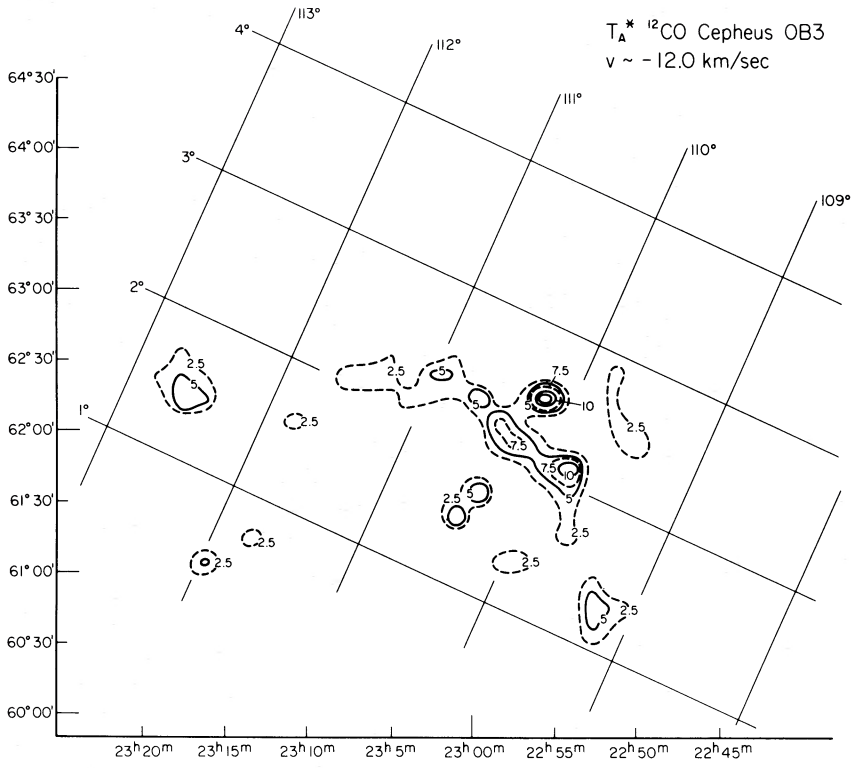

FIG. 4*a*.—Contours of $T_A^*(^{12}CO)$ measured at $V_{LSR} = -12.0$ km s^{-1}

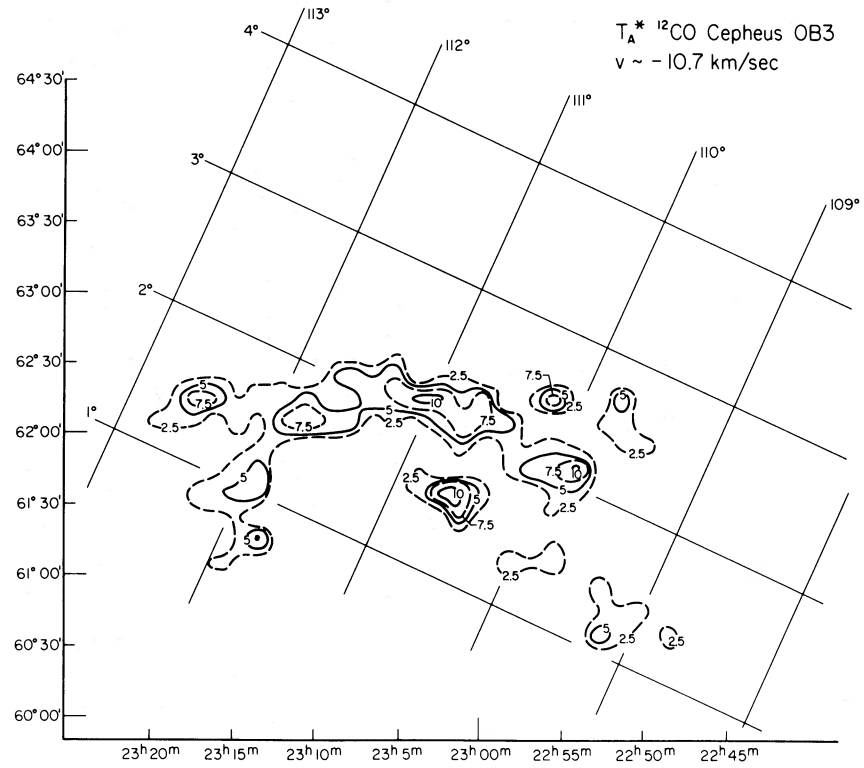

FIG. 4*b*.—Contours of $T_A^*(^{12}CO)$ at $V_{LSR} = -10.7$ km s^{-1}

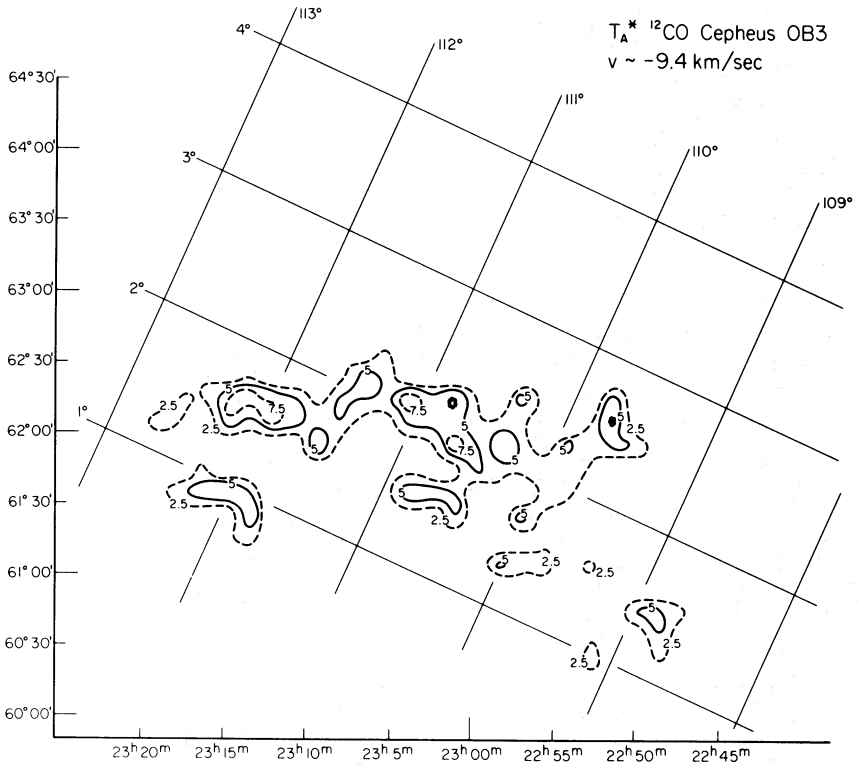

FIG. 4*c*.—Contours of $T_A^*(^{12}CO)$ at $V_{LSR} = -9.4$ km s^{-1}

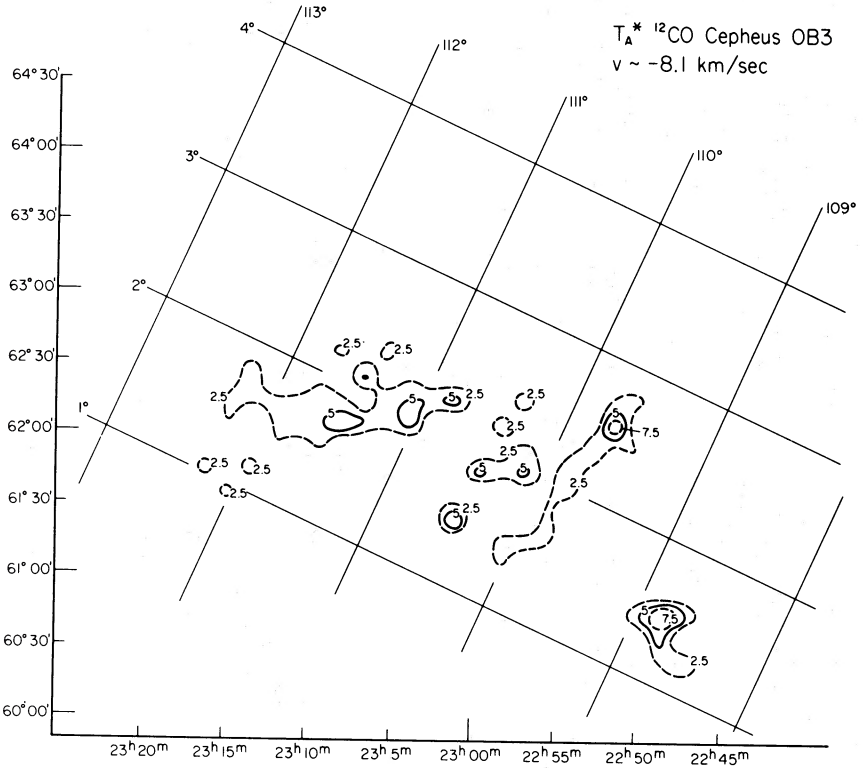

FIG. 4*d*.—Contours of $T_A^*(^{12}CO)$ at $V_{LSR} = -8.1$ km s^{-1}

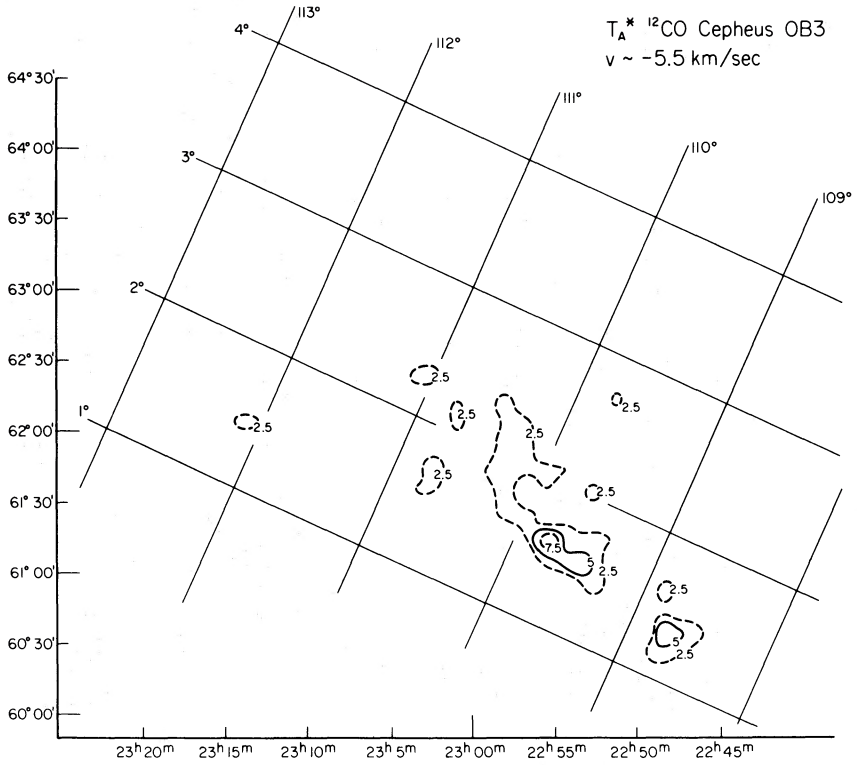

FIG. 4*e*.—Contours of $T_A^*(^{12}CO)$ at $V_{LSR} = -5.5$ km s^{-1}

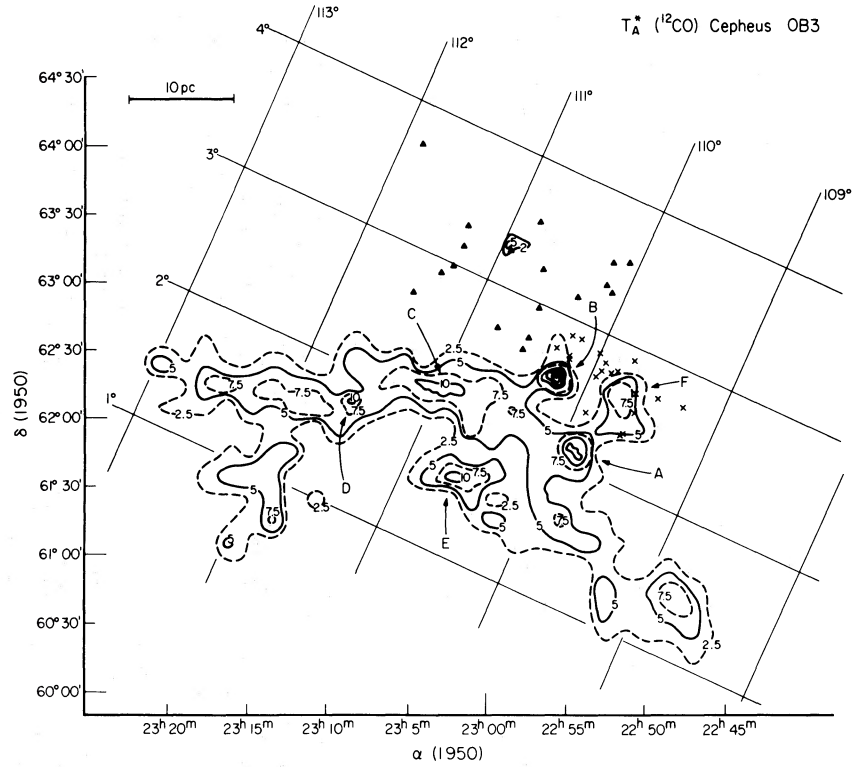

FIG. 4*f*.—Fig. 2 reproduced on same scale as Figs. 4*a*–4*e*.

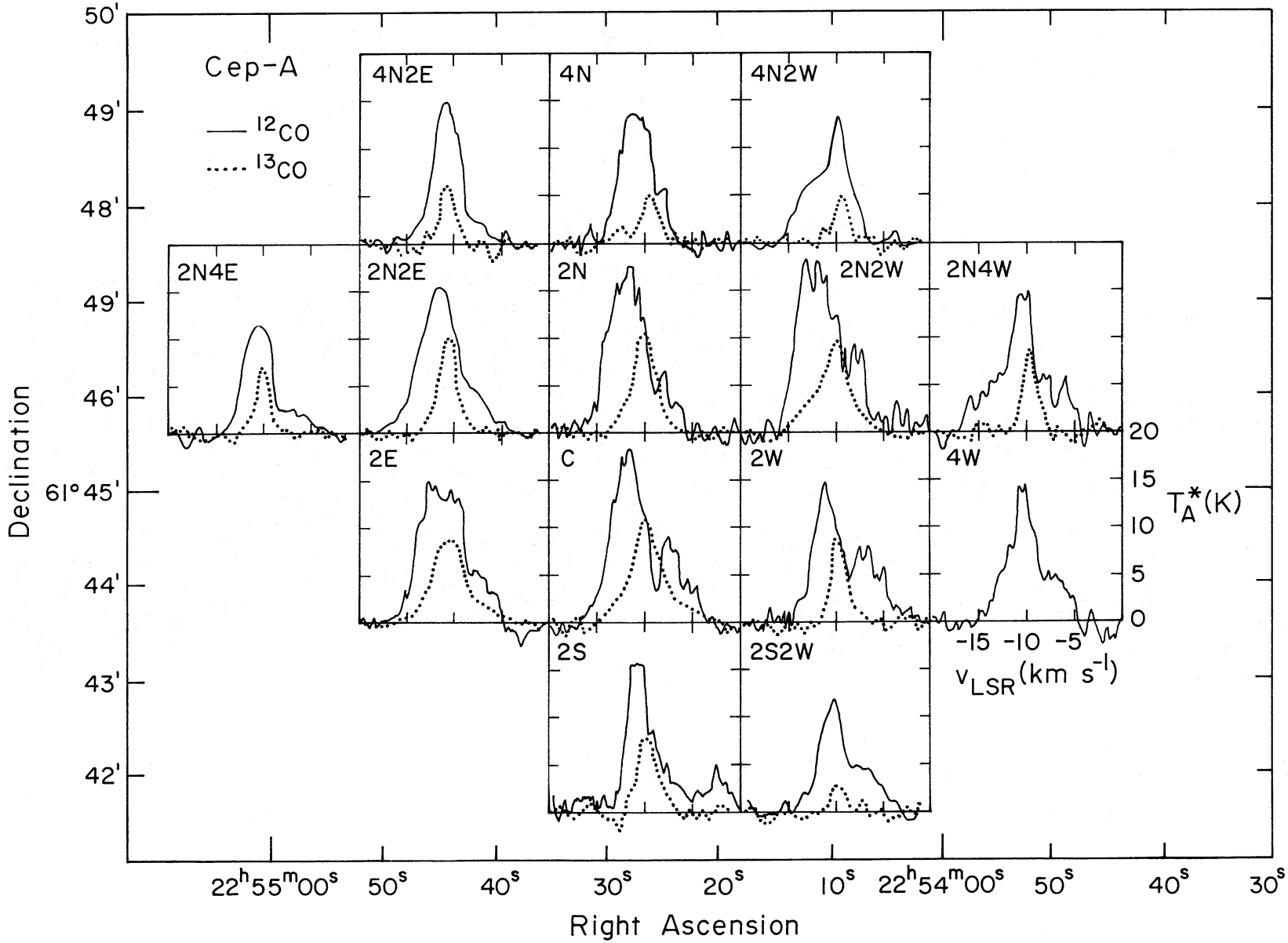

FIG. 5.—^{12}CO and ^{13}CO profiles observed about the central region of Cep A. 2W, 2N, etc., refer to observations 2′ west of center, 2′ north of center, and so on. The ^{12}CO profiles labeled 4N2E, 4N2W, 2N4E, 2N2E, and 2S2W, as well as all ^{13}CO data, are from the Aerospace 5 m. Other ^{12}CO data are from the 11 m NRAO instrument.

TABLE 2

OBSERVATIONS OF INDIVIDUAL REGIONS IN THE CEPHEUS OB3 CLOUD

	α(1950)	δ(1950)	^{12}CO T_A* (K)	^{12}CO [V_{LSR} (km s^{-1})]	^{13}CO T_A* (K)	^{13}CO [V_{LSR} (km s^{-1})]
Cep A.....	22^{h}54^{m}25^s	+61°44′36″	18:†	−12:†	11.0	−10.3
Cep B.....	22 55 27	+62 18 37	29.0	−12.3	8.1	−12.3
Cep C.....	23 03 38	+62 12 23	13.4	−10.3	9.1	−10.3

† Colon indicates approximate measurement.

Cep F imply that ^{13}CO is present to extents at least comparable with Cep B.

The velocity patterns of this isotope cannot be followed as closely as in § V*a*, since too few measurements are available. Moreover, the secondary features seen in ^{12}CO are rarely strong enough for equivalent ^{13}CO emission to be expected. Nevertheless, there is excellent agreement throughout the cloud between the velocities at which maxima in T_A*(^{12}CO) and T_A*(^{13}CO) appear. Although multiple lines are not detected from the rarer isotope at the positions where these are seen in ^{12}CO, weak and broad ^{13}CO features, encompassing the velocities of the various ^{12}CO emission peaks, are observed.

The ^{12}CO observations did not justify searches for ^{13}CO at stellar positions other than those given in Table 1. Detections were made at and around the locations of stars 11, 15, and 56, although the extent, as expected, was much less than that of ^{12}CO. The rarer isotope was also found near stars 2, 10, and 17. The velocity of peak T_A* is in all cases the same for both species.

The ^{13}CO data confirm the velocity structure implied by the ^{12}CO observations of the cloud complex and indicate the areas where density may be enhanced (see Paper III). In portions of the cloud closest to the association stars and to S155 (e.g., Cep B and Cep F), measurements of the rarer isotope are neither as intense nor as extended as in Cep A and Cep C (see § VI), where particularly broad ^{12}CO lines are found. Interpretation of these profiles as increased density indicators will be discussed in detail in Paper III.

c) H_2CO

Cep A, B, and C were examined for 140 GHz emission from H_2CO as described in § IV. At Cep A and Cep C 140 GHz H_2CO is unambiguously detected over areas approximately 6′ square, with maximum values of T_A*(H_2CO) ≈ 0.9 K and 0.6 K, respectively. The velocities of peak T_A*(H_2CO), being of the order of −10 km s^{-1}, are comparable with those of peak T_A*(^{12}CO) and T_A*(^{13}CO). It is doubtful that H_2CO is present at Cep B. This result may be related to the fact that values of T_A*(^{13}CO) observed there were considerably lower than those found at Cep A and Cep C.

VI. DETAILED STUDIES OF CEPHEUS A, CEPHEUS B, CEPHEUS C

The regions Cep A, B, and C were observed at higher resolution in ^{12}CO and examined for the presence of ^{13}CO and H_2CO as described in §§ III and IV. Relevant parameters for each region are presented in Table 2.

a) *Cepheus A*

Perhaps the most interesting portion of the Cepheus OB3 cloud complex is Cep A. In Figure 5 are shown the ^{12}CO and ^{13}CO line profiles observed around the center of the zone. Over a small region these profiles are characterized by deep minima, possibly the result of self-absorption. The variation of this phenomenon with position is clearly illustrated. Note that the ^{12}CO profiles were obtained with a different instrument and at higher resolution than their ^{13}CO equivalents. Contours of T_A*(^{13}CO) are displayed in Figure 6. Because interpretation of the ^{12}CO profiles is complicated by the absorption feature, no equivalent contours of T_A*(^{12}CO) are presented.

From Figure 5 it is evident that the absorption feature is present only in the immediate vicinity of the central position; the ^{12}CO intensity minimum lies at −8.8 km s^{-1} and the ^{13}CO maximum at −10.3 km s^{-1}. Where the feature is absent, the ^{12}CO and ^{13}CO maxima appear at the latter velocity. Displacement to yet more negative velocities of the ^{12}CO maxima at positions north and east of center is attributable to the presence of an additional component at ∼ −12 km s^{-1}. The 2 mm H_2CO lines observed at Cep A are shown in Figure 7. Usually the velocity of the H_2CO maximum is the same as that of the ^{13}CO peak at the same position, but a component at ∼ −12 km s^{-1} is clearly present at the central position. When Figures 5 and 7 are compared, it is clear that in Cep A the presence of a ^{12}CO absorption feature is well correlated with the detection of 2 mm H_2CO.

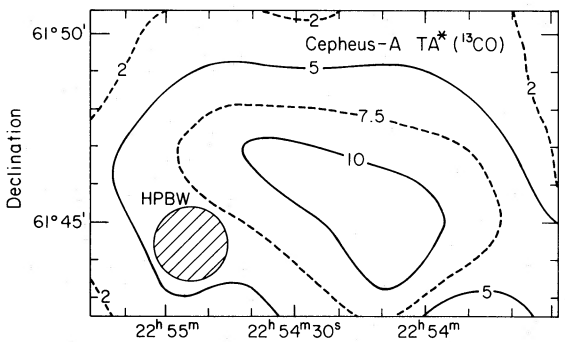

FIG. 6.—Contours of T_A*(^{13}CO) at V_{LSR} = −10.3 km s^{-1} for Cep A.

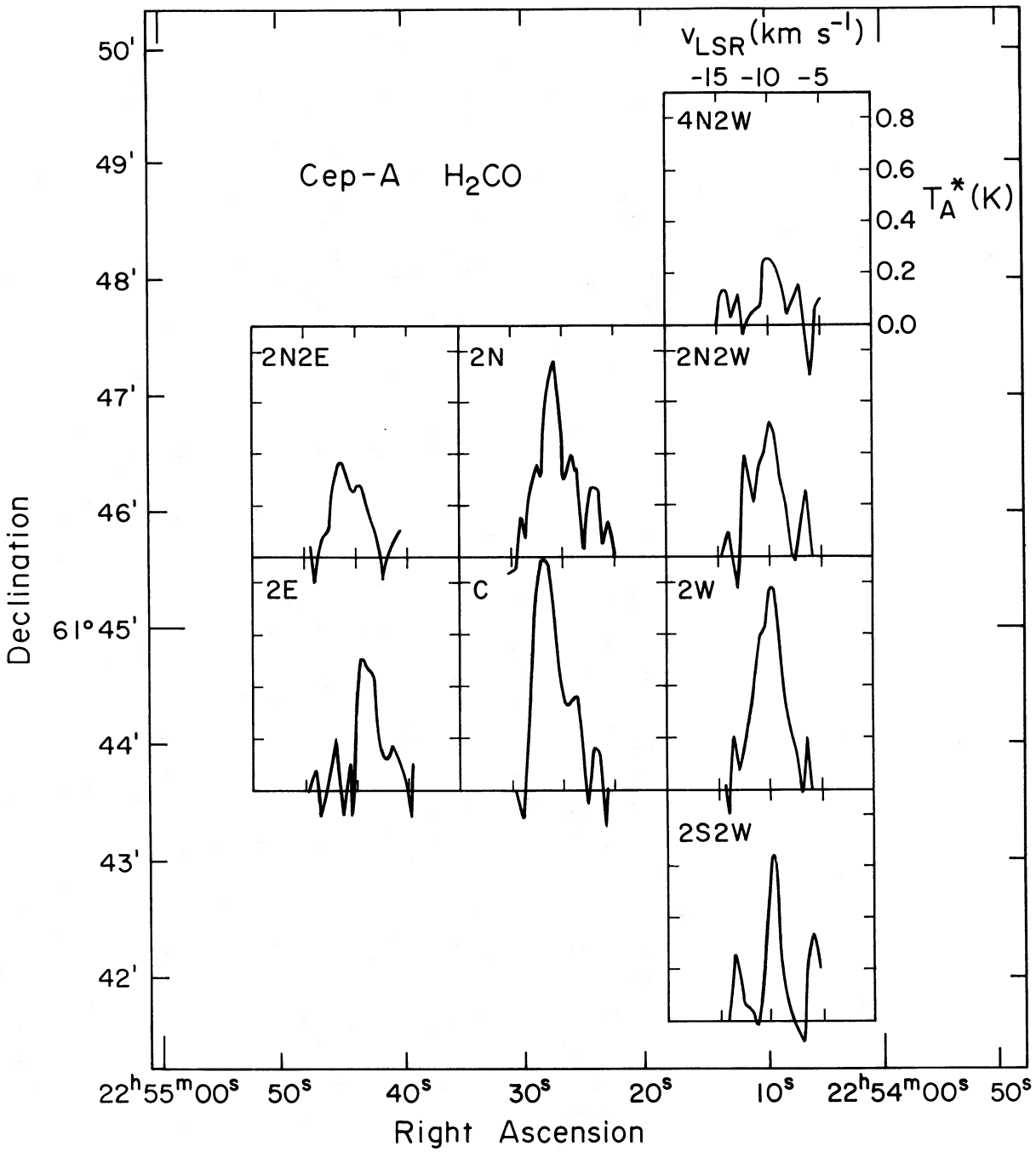

FIG. 7.—H_2CO profiles observed over the central region of Cep A

b) Cepheus B

The highest values of $T_A^*(^{12}CO)$ in the Cepheus OB3 cloud are found in Cep B. The position is marked by a cross in Figures 8*a* and 8*b*, where contours of $T_A^*(^{12}CO)$ and $T_A^*(^{13}CO)$, respectively, are shown. Emission from Cep B is primarily at -12.0 km s^{-1}, although, at the boundary of the cloud itself (see Fig. 2), a feature at ~ -15 km s^{-1} remarked upon in § V is evident. Over the whole region the ratio $T_A^*(^{12}CO)/T_A^*(^{13}CO)$ is 3–5, and the ^{12}CO lines have widths at half-maximum of between 2 and 4 km s^{-1}. Limited searches of the region have been made in the 2 mm line of H_2CO, but no detections have resulted.

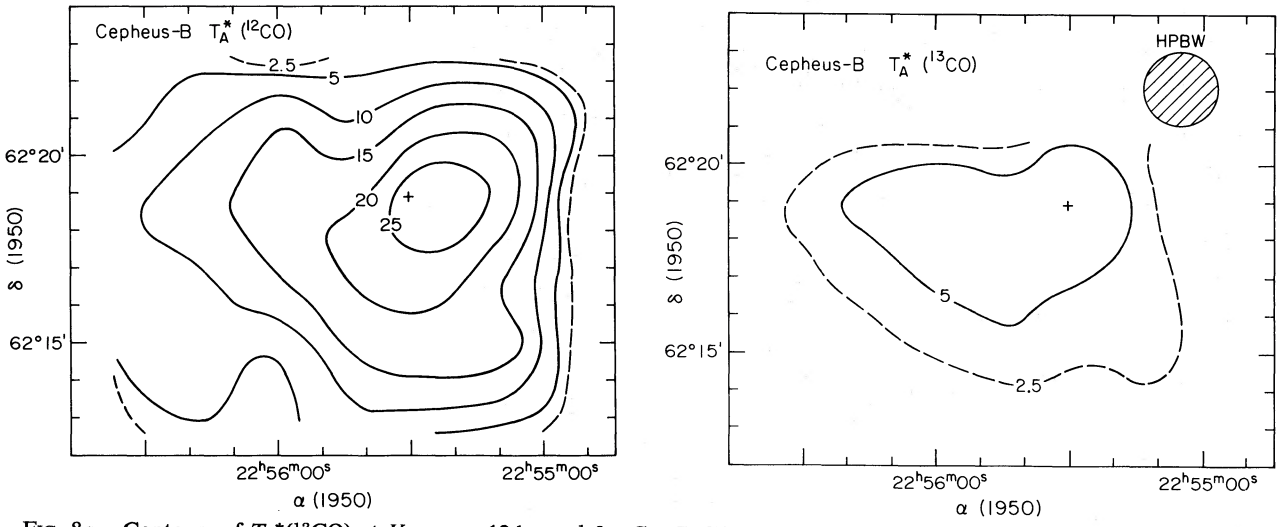

FIG. 8*a*.—Contours of $T_A^*(^{12}CO)$ at $V_{LSR} = -12$ km s^{-1} for Cep B. The cross indicates the position of maximum $T_A^*(^{12}CO)$.
FIG. 8*b*.—Contours of $T_A^*(^{13}CO)$ at $V_{LSR} = -12$ km s^{-1} for Cep B. A cross indicates the position of maximum $T_A^*(^{13}CO)$.

c) Cepheus C

Several velocity components are visible in the ^{12}CO profiles observed across Cep C (see Figs. 4*a*, *b*, *c*, *d*). Over most of the region only one of these components, that at -10.3 km s^{-1}, is also seen in ^{13}CO. Contours of $T_A^*(^{12}CO)$ and $T_A^*(^{13}CO)$ are presented in Figures 9*a* and 9*b*. Maximum values of these quantities occur at different, although adjacent, positions, as can be seen from the figures. The core of Cep C probably encompasses both maxima, since unambiguous detections of 2 mm H_2CO were made at their positions. From Table 2 it is clear that, in view of the observed $T_A^*(^{12}CO)$, the values of $T_A^*(^{13}CO)$ are unexpectedly high.

To the north and west of the central position shown in Figure 9*a*, a feature at -11.7 km s^{-1} gradually increases in strength. This northwest zone is in fact not unlike Cep B in its general properties. Few ^{13}CO observations were made here, since it is relatively far from the site of peak intensity, $\alpha = 23^h03^m38^s$, $\delta = +62°12'23''$, but existing measurements indicate that the rarer isotope is never more than weakly present.

VII. SUMMARY

Detailed discussion and interpretation of the observations presented in this paper will be undertaken in Paper III. At this juncture the data will merely be summarized and indications will be given of the direction the analysis will take.

It has been demonstrated that in the vicinity of the young OB association Cepheus OB3 there is a large (20 pc × 60 pc) molecular cloud complex comprising a number of components, several of which overlap in the line of sight. Emission from these components is seen at a number of velocities between -5 km s^{-1} and -15 km s^{-1}. Such velocities lie well within the range spanned by the association stars and the H II region S155, confirming the relationship between the cloud complex and the OB association.

Within this molecular cloud, from which Cepheus OB3 appears to have formed, three regions, Cep A, B, and C, have particularly interesting properties. The interpretation of self-absorption profiles such as those seen in the direction of Cep A is at present under discussion (Snell and Loren 1977; Leung and Brown 1977). It appears, however, that such profiles are

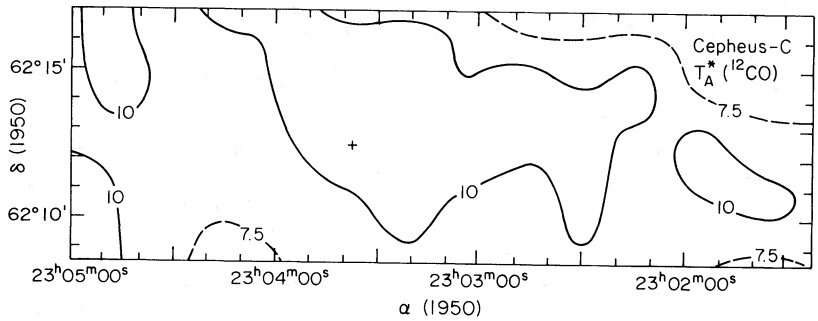

FIG. 9*a*.—Contours of $T_A^*(^{12}CO)$ at $V_{LSR} = -10.3$ km s^{-1} for Cep C. The cross indicates the position of maximum $T_A^*(^{12}CO)$.

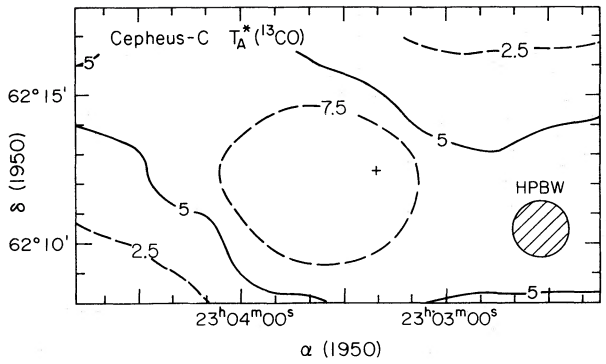

FIG. 9*b*.—Analogous contours of ^{13}CO. A cross indicates the position of maximum $T_A^*(^{13}CO)$.

observed at locations where new stars are currently forming. Intensity ratios and line widths over Cep B are typical of dark clouds heated by a single star (Milman *et al.* 1975*a*, *b*; Dickman 1975). Simonson and van Someren Greve (1976) did in fact detect, in the direction of Cep B, a small H I concentration which they concluded lay in front of S155 and was related to the dark clouds around Cepheus OB3. Observations in this direction made with the Westerbork Synthesis Radio Telescope at a wavelength of 6 cm indicate the presence of a weak extended ($\sim 30''$) H II region suggestive of an early B star (Israel 1977), but no other evidence for the existence of such a source in the form, for example, of an infrared object has been discovered. Searches (to 10 Jy sensitivity) within each region for H_2O masers at the positions of peak ^{12}CO intensity have yielded no detections (Knapp 1977).

Thus in the Cepheus cloud complex there is some evidence for the existence of an embedded star (Cep B), a region of continuing star formation (Cep A), and a zone, Cep C, which is perhaps the precursor of regions such as Cep A and Cep B.

It is clear that there is indeed a large amount of gas still associated with the stars of Cepheus OB3. Estimates of its mass relative to the member stars and neutral hydrogen in the association are of primary importance in considering the evolution of the complex. In view of the quantities of data involved and the very careful analysis necessary to determine the precise relationship between the association and the molecular cloud, the interpretation of the observations will be deferred until Paper III.

I appreciate very much the generous spans of observing time allocated me at the Aerospace Corporation by E. E. Epstein. Observing time at the Millimeter Wave Observatory and the National Radio Astronomy Observatory is also gratefully acknowledged. I am indebted to G. R. Knapp for introducing me to the technicalities of millimeter radio astronomy and to S. Beckwith, T. Boroson, P. Vanden Bout, J. Elias, N. J. Evans, P. Goldreich, G. Neugebauer, R. N. Snell, J. D. White, and W. J. Wilson for assistance at various stages of the project.

REFERENCES

Becklin, E. E., Neugebauer, G., and Wynn-Williams, C. G. 1973, *Ap. J.* (*Letters*), **182**, L7.
Beckwith, S., Evans, N. J., II, Becklin, E. E., and Neugebauer, G. 1976, *Ap. J.*, **208**, 390.
Blaauw, A. 1964, *Ann. Rev. Astr. Ap.*, **2**, 213.
Blaauw, A., Hiltner, W. A., and Johnson, H. L. 1959, *Ap. J.*, **130**, 69.
Crawford, D. L., and Barnes, J. V. 1970, *A.J.*, **75**, 952.
Dickman, R. L. 1975, *Ap. J.*, **202**, 50.
Downes, D., Winneberg, A., Goss, W. M., and Johansson, L. E. B. 1975, *Astr. Ap.*, **44**, 243.
Elmegreen, B. C., and Lada, C. J. 1977, *A.J.*, **81**, 1089.
Garmany, C. 1973, *A.J.*, **78**, 185.
Garrison, R. F. 1970, *A.J.*, **75**, 1001.
Georgelin, Y. M. 1975, Ph.D. thesis, Université de Provence, Observatoire de Marseilles.
Harris, S. 1976, Ph.D. thesis, University of Cambridge.
Harris, S., and Wynn-Williams, C. G. 1976, *M.N.R.A.S.*, **174**, 649.
Israel, F. P. 1977, private communication.
Kester, D. 1977, private communication.
Knapp, G. R. 1977, private communication.
Kutner, M. L., and Tucker, K. D. 1975, *Ap. J.*, **199**, 79.
Lada, C. J. 1976, *Ap. J. Suppl.*, **32**, 603.
Leung, C. M., and Brown, R. L. 1977, *Ap. J.* (*Letters*), **214**, L73.
Limber, D. N. 1960, *Ap. J.*, **131**, 168.
Liszt, H. S., Wilson, R. W., Penzias, A. A., Jefferts, K. B., and Wannier, P. G. 1974, *Ap. J.*, **190**, 557.
Lucas, R., Encrenaz, P. J., and Falgarone, E. G. 1976, *Astr. Ap.*, **51**, 469.
Mezger, P. G., and Wink, J. E. 1975, in H II *Regions and Related Topics*, ed. T. L. Wilson and D. Downes (New York: Springer-Verlag), p. 408.
Miller, J. S. 1968, *Ap. J.*, **151**, 473.
Milman, A. S., Knapp, G. R., Kerr, F. J., Knapp, S. L., and Wilson, W. J. 1975*a*, *A.J.*, **80**, 93.
Milman, A. S., Wilson, W. J., Knapp, G. R., and Knapp, S. L. 1975*b*, *A.J.*, **80**, 101.
Sargent, A. I. 1978*a*, in preparation (Paper II).
———. 1978*b*, in preparation (Paper III).
Simonson, S. C., and van Someren Greve, H. W. 1976, *Astr. Ap.*, **49**, 343.
Snell, R. L., and Loren, R. B. 1977, *Ap. J.*, **211**, 122.
Ulich, B. L., and Haas, R. 1976, *Ap. J. Suppl.*, **30**, 247.
Zuckerman, B., and Palmer, P. 1974, *Ann. Rev. Astr. Ap.*, **12**, 279.

ANNEILA I. SARGENT: Department of Astronomy 105-24, California Institute of Technology, Pasadena, CA 91125